

T-61.181 Special course in Information Science I
Time in Self-Organizing Maps
SOTPAR and SOTPAR2

Tom Bäckström (43102M)
Helsinki University of Technology
Laboratory of Acoustics and Audio Signal Processing
P.O.Box 3000, FIN-02015 Finland
tom.backstrom@hut.fi

November 15, 2002

1 Preface

This paper is a summary of a selection of papers on a method called Spatio-Temporal Self-Organizing Feature Maps (SOTPAR) [1, 2, 3, 4]. Further, we will assume that the reader is familiar with the basics of self-organizing maps.

2 The Spatio-Temporal Self-Organizing Feature Map (SOTPAR) Model

The SOTPAR model is based upon a traveling wave through the nodes of a Self-Organizing Feature Map (SOFM), which progresses from each winner in a predetermined “time” direction. That is, in the 2D-case, the wave travels in time along the surface of the map in a specified direction. In the one dimensional case, the wave travels (for example), left to right, which gives the following equation for temporal activity

$$\text{temp}_i(t) = \lambda^{\|i, \text{win}(t_0)\|} (1 - \lambda)^{t - t_0 - \|i, \text{win}(t_0)\|} u(t - t_0 - \|i, \text{win}(t_0)\|), \quad (1)$$

where λ is the attenuation factor, $\|i, \text{win}(t_0)\|$ the distance between node i and the winning node at time t_0 and $u(\cdot)$ the unit step function. See Fig. 1 for a demonstration in the one dimensional case and Fig. 2 for the corresponding flow-graph. For higher order systems, the wave front can be allowed to move in diagonal directions as well, but according to our definition it always moves to the right. A demonstration of the memory-kernel is depicted in Fig. 3.

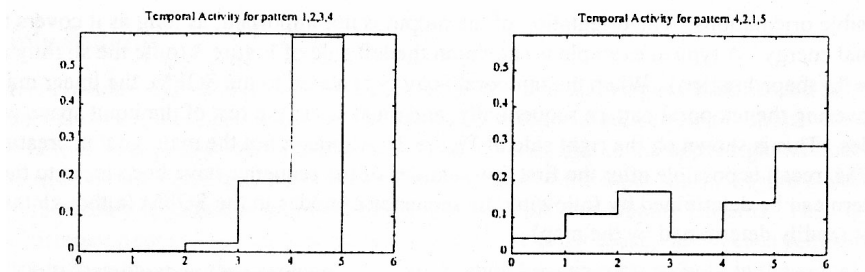


Figure 1: Temporal activity created in the network by temporally ordered or unordered input.

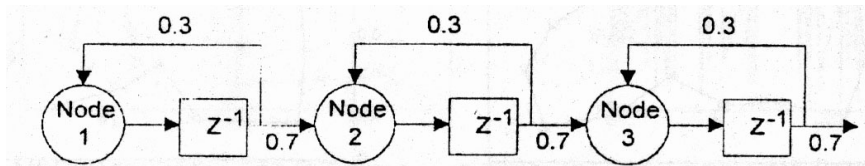


Figure 2: One-dimensional coupling of SOFM nodes for spatio-temporal activity.

Training of the SOTPAR model is simple and very similar to the regular SOFM model. The two stages are very much alike SOFM: Firstly, find the winning node,

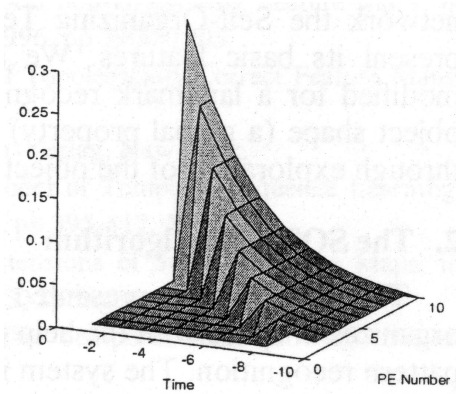


Figure 3: Memory-kernel for SOTPAR.

and secondly, update the neighborhood weights of the winning node. The second step is equal to SOFM, but in the first stage we add a temporal weighting to the winning criterion. The winner is selected with the following formulas

$$\text{win}(t) = \arg \min_{1 \leq j \leq N} [\|x, \mathbf{w}_j\| - \beta \cdot \text{temp}_j(t)] \quad (2)$$

$$\begin{aligned} \text{temp}_j(t) = & \lambda \cdot [\text{temp}_j(t-1) + \delta_{j, \text{win}(t-1)}] \\ & + (1 - \lambda) \cdot [\text{temp}_{j-1}(t-1) + \delta_{j-1, \text{win}(t-1)}], \quad (3) \end{aligned}$$

where β is the Temporal/Spatial Proportion (TSP) parameter, λ defines the temporal decay and δ is the Kronecker delta function.

3 Simulation

As a first experiment, a simple toy-example was constructed. The input data was uniformly distributed data on $[0, 1] \times [0, 1]$ which was concatenated with a 20 sample 'L'-shaped figure (from $[0.5, 1.0] \rightarrow [0.5, 0.5] \rightarrow [1.0, 0.5]$) with additive uniform noise (between ± 0.05).

This input sequence was trained on a regular SOFM and the proposed SOTPAR model. A demonstration of the results is depicted in figure 4. The results show that whereas SOFM does not catch the temporal 'L'-shape, SOTPAR does a good job finding that sequence. In addition, both models cover the whole space adequately.

Continuing with a slightly more difficult task, the input data was altered so that the 'L'-shaped sequences were time-warped (shrunk and stretched) up to 50%. The results are shown in Fig 5. The desirable properties are successfully maintained, that is, the test sequence is still correctly temporally mapped. Notice also how the sequence of winners catches the temporal data.

Finally, the experiment was extended to include two, overlapping 'L'-shaped figures. Results are shown in Fig. 6. It is obvious that while the input data becomes more complex, the model will also become more complex. However, both sequences are clearly found even though the model has a discontinuity in the lower left corner 'L'-figure. In addition, the two 'L'-shaped figures have now seemingly become dominant

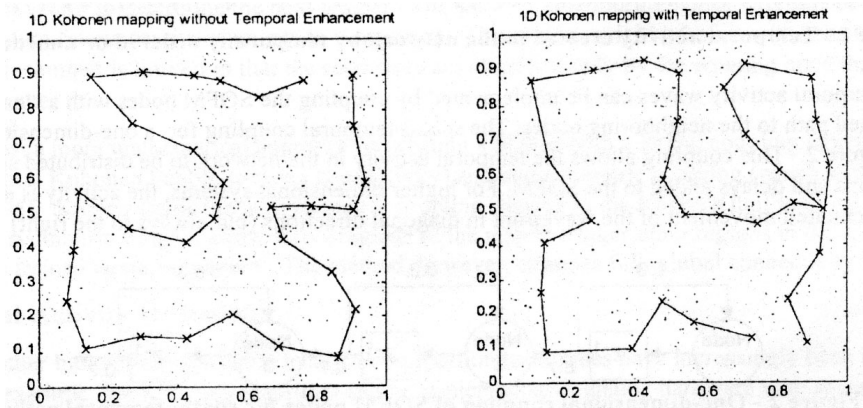


Figure 4: One-dimensional mapping of a two-dimensional input space with an embedded 'L'-shaped figure.

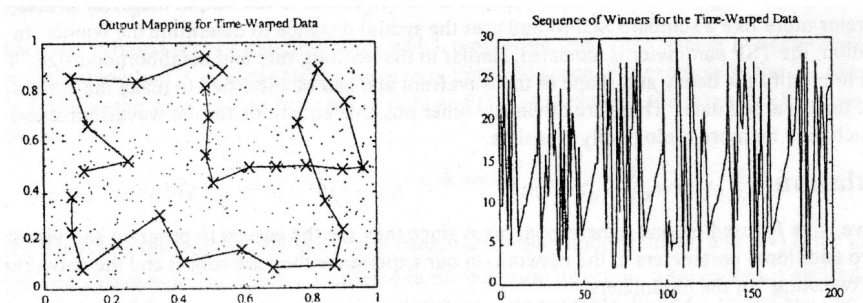


Figure 5: One-dimensional mapping of a two-dimensional input space with embedded time-warped 'L'-shaped figures.

in the input space in such an extent that the rest of the space obtains a small number of nodes only.

4 Application to Robot Landmark Recognition

Consider the problem of a robot recognizing landmarks with infra-red sensors. The field of view is limited (approx. 10 degrees) and close range. The movements of the robot are sluggish and the exact position is unknown. The task is to recognize landmark objects by moving around them by the wall from an unknown starting point. The turning points (corners of the object) and travelling times between them are the features.

In a simulation of this problem, we have two training objects (see Fig. 7) an 'L'-shaped figure and a square. Two maps are trained, one for each object, and in the recognition test, the map that stabilizes at a higher activity level wins. See Fig. 7 for results. When the robot starts travelling around the object, both maps obtain similar activity levels. Since there are two differences in the objects (the 'L'-shaped figure has two more corners), the map trained with squares will find unlikely features and stabilize at a lower activity level. It is evident that each time the map trained with

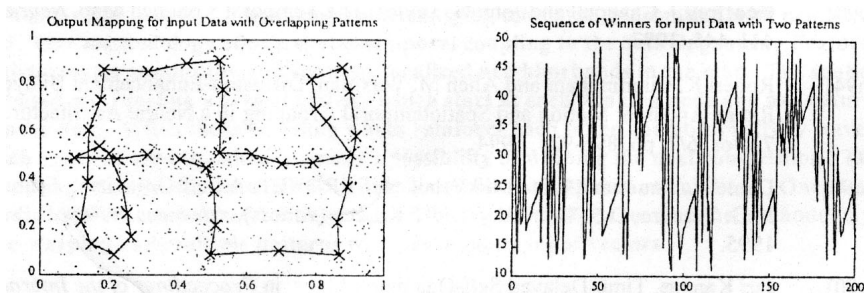


Figure 6: One-dimensional mapping of a two-dimensional input space with multiple embedded 'L'-shaped figure.

squares reaches the “wrong” turning point in the 'L'-shape, the activity level drops, until familiar features are once again found and the activity level rises. Since the two shapes are so similar, this should have been a difficult problem. Nevertheless, the model solves the problem quite elegantly. However, this approach requires multiple circumnsions of the landmark object since the robot does not have any way of knowing when it has reached its starting point. This could be avoided with external logic to identify completion of a full round, and then inputting repeatedly the data of the single round subsequently to the map. However, the noise present in the single round would then play a significant role in the task, a role that might be diminished with several round around the object.

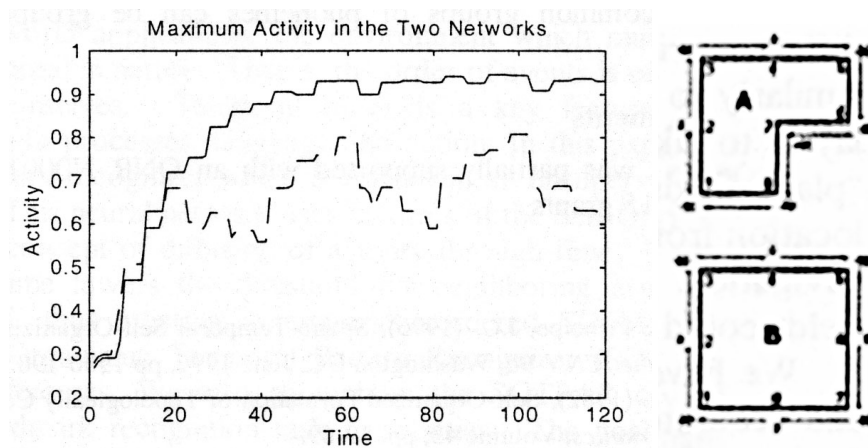


Figure 7: Maximum activity levels of two networks trained for an 'L'-shaped figure and a square, exited with an 'L'-shaped figure. The solid line denotes activity of map trained with the 'L'-shape, dashed line the square figure.

5 SOTPAR2

In SOTPAR2 the idea of SOTPAR is generalized so that the temporal direction in the map is relaxed to modification as subject to training. The temporal activity is now

defined by

$$\text{temp}_i(t+1) = \alpha \text{temp}_i(t) + \frac{\sum_k \{ [\mu f(\mathbf{d}, k) + (1 - \mu) \text{temp}_k(t)] p_{k,i} \}}{\max(p)}, \quad (4)$$

where $\text{temp}_i(t)$ is the temporal activity at node i at time t , α is a decay constant less than 1, $p_{i,j}$ the connection strength from node i to j , μ a parameter which smoothes the activity giving more or less importance to the past activity in the network and $\max(p)$ a normalisation coefficient. Function $f(\cdot)$ relates the how the current match contributes to the activity, and \mathbf{d} is a vector of distances d_i to each node i .

This design implies that previous winners all affect the output activity of the current winner. Known paths through the map will therefore get higher selection probability at the next round. If the data has followed a known path but deviates from it temporarily, the wave will continue along the path in case the data would soon return to that path. This also implies that the Voronoi regions of each node change according to previous winners, that is, the Voronoi region of a node corresponding to the next element in a known path will be significantly larger than when travelling along some other path or no path at all. This property is demonstrated in Fig. 8.

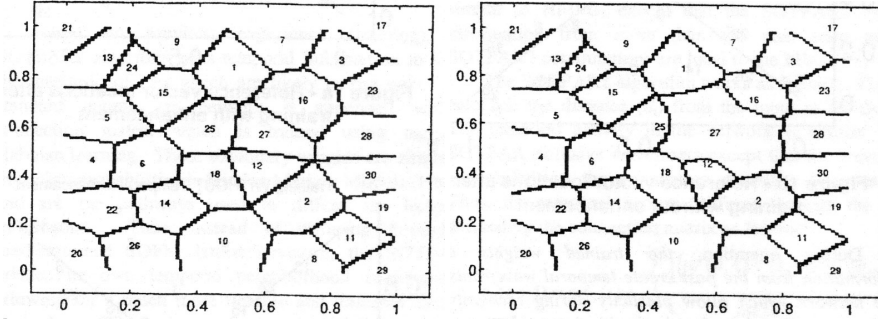


Figure 8: The Voronoi region of elements when previous inputs are not on a known path (left figure) and when previous inputs are on a path leading to element 27 (right figure).

6 Discussion

We have, in previous presentations, seen many different types waves along the surface of SOF maps. The method studied in this paper, Spatio-Temporal Self-Organizing Maps, are different in the sense that the waves propagate in a specified direction (SOTPAR) or in a direction regulated by self-organization (SOTPAR2). One question that was left open in the presented material is behaviour of maps when the input propagates along a known path faster than any of the training data. One would expect that this would produce a severe failure in recognition. However, all the presented simulations showed encouraging results.

References

- [1] N. R. Euliano and J. C. Principe, "Spatio-temporal self-organizing feature maps," in *Proc. Int. Joint Conf. on Neural Networks (IJCNN'96)*, Washington, DC, 1996, vol. 4, pp. 1900–1905.
- [2] N. R. Euliano, J. C. Principe, and P. Kulzer, "A self-organizing temporal pattern recognizer with application to robot landmark recognition," in *Spatiotemporal Models in Biological and Artificial Systems*, F.L Silva et al., Ed., pp. 41–48. IOS Press, 1997.
- [3] N. R. Euliano and J. C. Principe, "Temporal plasticity in self-organizing networks," in *Proc. World Cong. on Computational Intelligence (WCCI'98)*, 1998, pp. 1063–1068.
- [4] N. R. Euliano and J. C. Principe, "A spatio-temporal memory based on soms with activity diffusion," in *Kohonen Maps*, E. Oja and S. Kaski, Eds., pp. 253–265. Elsevier Science B. V., 1999.